

# Development of Electromagnetic Tomography (EMT) for Industrial Applications. Part 2: Image Reconstruction and Software Framework

A R Borges<sup>1</sup>, J E de Oliveira<sup>1</sup>, J Velez<sup>1</sup>, C Tavares<sup>1</sup>, F Linhares<sup>1</sup>, A J Peyton<sup>2</sup>

<sup>1</sup> INESC-Aveiro, Portugal, ruib@inesca.inesca.pt

<sup>2</sup> Engineering Department, Lancaster University, UK, a.peyton@lancaster.ac.uk

**Abstract** – This paper is the second of two parts and reviews results of a recently completed project based at the University of Aveiro, UMIST and the University of Lancaster. This research represents a fundamental investigation of the potential of using electromagnetic inductance measurements for industrial tomographic applications.

This second paper concentrates on image reconstruction and software related issues and follows on from hardware related topics described in the first part. The systems studied can image the distribution of either electrically conducting material ( $s > 1$  S/m) and / or magnetically permeable materials ( $\mu_R > 1$ ). The technique has analogies with other forms of electrical tomography such as those based on resistance or capacitance methods. The paper describes several general approaches to image reconstruction, the development of particular image reconstruction algorithms, and the performance of the system in terms of image resolution and image capture and reconstruction rates. The system is controlled from a distributed software framework, which is also presented briefly. Finally a number of potential industrial applications for the EMT technique are discussed.

**Keywords** : Sensors, Tomography, Electromagnetic inductance, Image reconstruction

## 1. INTRODUCTION

For electrical tomography systems, such as EMT, the reconstruction problem is complicated by the soft field effect, whereby the object material changes both the magnitude and direction of the interrogating field. The basic physical principles involved in EMT are described by Maxwell's equations. For the two dimensional case (x-y plane), we can make a number of assumptions such as ignoring the effects of the displacement current which may be negligible for the materials and signal frequencies,  $\omega$ , of interest ( $\omega \ll s$ ). Free charges can be neglected and the material can be assumed to have linear and isotropic electrical and magnetic properties. Then using complex vector notation, we have,

$$\nabla \times \left[ \left[ \nabla \times \frac{\mathbf{B}_{x,y}}{\mathbf{m}_{x,y}} \right] / \mathbf{s}_{x,y} \right] = -j\omega \mathbf{B}_{x,y} \quad \nabla \cdot \mathbf{B}_{x,y} = 0 \quad (1)$$

and for the coil windings,

$$\nabla \times \mathbf{B}_{x,y} = \frac{\mathbf{J}_{app}}{\mathbf{m}_0} \quad \nabla \cdot \mathbf{B}_{x,y} = 0 \quad (2)$$

where,  $\mathbf{B}_{x,y}$  is the magnetic flux density vector and  $\mathbf{J}_{app}$  is the applied current density in the windings of the coil array. It is convenient to introduce the magnetic vector potential  $\mathbf{A}$  and electric scalar potential  $\phi$ , using the gauge,

$$\mathbf{H} = \nabla \times \mathbf{A} \quad \mathbf{E} = j\omega \mathbf{m} \mathbf{A} - \nabla \phi \quad (3)$$

Combining these equations and using well know vector identity results in a scalar Helmholtz equation.

$$\nabla^2 \mathbf{A} = j\omega \mathbf{m} \mathbf{A} \quad (4)$$

Note that (3) describes the general case; the problem is not fully described until the boundary conditions are also included. These are specific to the sensor geometry, applied excitation current and the regions of different object materials.

The spatial distribution of the magnetic field and hence the mutual coupling between the coils is altered by the introduction of object material which either is ferro/ferrimagnetic ( $\mu_R > 1$ ) and / or has a high electrical conductivity. Figure 1 illustrates these basic electromagnetic effects for different materials and gives a visual impression of character of the soft field effect. In this example, a target object (diameter 40mm) is placed in an 8-pole EMT sensor (object space 200 mm). In simple terms, if the target object is magnetic and non-conducting then the magnet flux flow preferentially thought the object. This is shown in Figure 1(c) and overall the mutual coupling between the coils increases, resulting in increased measurements. Alternatively if the object is non-magnetic and conducting then the flux in the object is reduced due to induced eddy currents, and overall the

measurements are also reduced. This situation is shown in Figure 1(d) for an aluminium target, with a 100 kHz excitation frequency. Here, the skin effect prevents virtually any penetration of the applied field into the target. Finally a material, which is both magnetic and conductive, displays both effects and the skin layer of the objects acts as a preferential path to the flow of flux.

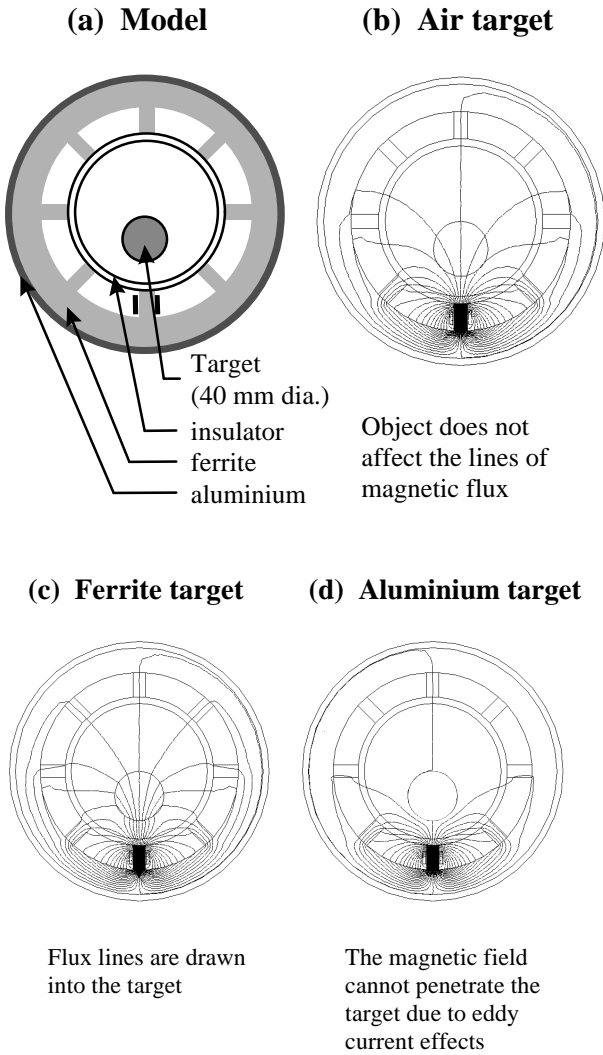


Figure 1: EMT and the soft field effect

## 2. IMAGE RECONSTRUCTION

The solution to the inverse problem presents formidable difficulties and is still the subject of much research. Some of the more popular approaches [29-32] to solving this problem are summarised in Table 1.

Type / Algorithm	Comments
<b>Rule based</b>	
Parameter extraction	A priori knowledge must be assumed.
Object classification	This involves applying simple formulae or rules directly to the raw data from the sensor in order to determine particular quantities, e.g. level of liquid in a tank, size type of material (Al, Fe, or ferrite) and position of a single object, etc.
<b>Qualitative - direct</b>	
Back-projection	Very little practical application to EMT.
Weighted back-projection	Modified version of back-projection where the measured values are projected back along the curved field contours. The field contours are taken to be the empty space or uniform case, e.g. [1, 2]
Sensitivity coefficient	<p>The reconstruction calculation is arranged in matrix format as follows,</p> $p \approx A.f$ <p>where, <math>p</math> is the measurement vector, <math>f</math> is the image pixel values arranged in a vector and <math>A</math> describes the physical model of the sensor and acquisition system. Note, linearity is assumed and object interactions are neglected. <math>A</math> cannot be inverted. So an approximate process of taking, <math>S</math>, where</p> $s_i = \frac{a_i^T}{\ a_i^T\ ^2}$ <p>is often used for reconstruction in</p> $f = S.p$ <p>The coefficients in <math>A</math> can be found by FE simulation, or by direct measurement with known perturbations, e.g. [3].</p>
NOSER	<p>One iteration Newton-Raphson is a single matrix multiplication approach, whereby a more effective estimation of <math>S</math> is used than the simple transpose approach above.</p> $p \approx A.f \quad A^T.p \approx [A^T.A]f$ <p>i.e. <math>f \approx [A^T.A]^{-1}.A^T.p</math></p> <p>Note, <math>[A^T.A]</math> requires regularisation to either make the inversion possible or to reduce numerical inaccuracies using <math>[A^T.A] \rightarrow [A^T.A + \mu I]</math> and <math>\mu</math> must be optimised for each system.</p>
<b>Qualitative - iterative</b>	
Arithmetic Reconstruction Techniques (ART)	Arithmetic Reconstruction Technique [4,5] is similar to SIRT but with a different updating procedure. New pixel values are updated as they are calculated. Faster than SIRT but generally more sensitive to noise.
Simultaneous Increment Reconstruction Technique (SIRT)	Iterative approach whereby an initial guess of the image is made. The measurements are then calculated using $p_{calc} \approx A.f$ and the error between the calculated and the actual measurements are obtained using $p_{error} = p_{meas} - p_{calc}$ . An error image can then be obtained using the sensitivity coefficient method $f_{error} = S.p_{error}$ and used to improve the estimate of the image. The process is iterated until a pre-set limit or the errors are sufficiently small.

Type / Algorithm	Comments
<b>Quantitative</b>	
Finite Element (FE) based	Widely used for EIT e.g. [6,7] and more recently for ECT [8,9]. Typical implementation uses an iterative method based on a FE model to calculate the sensor outputs, which are then compared with the actual, measured sensor outputs. The estimated material distribution is then updated using a modified Newton-Raphson approach. The recent work on ECT uses a control loop analogy for this iterative process.
<b>Heuristic</b>	
Neural network	Learning based algorithms where the algorithm is first trained with sets of measurements and corresponding images [10].

Table 1: Summary of reconstruction algorithms Used for electrical tomography

In general, there is a trade-off between the computational complexity of the algorithm and the quality of the images generated as shown in Figure 2. However, the best algorithm for a particular situation depends very much on the exact nature of the problem, on the characteristic of the material involved and whether any a priori knowledge can be assumed.

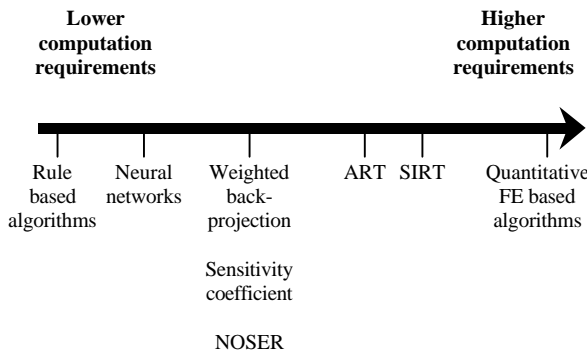


Figure 2: Relative computational requirements of various algorithms

Most of the reconstruction algorithms described in the previous table have been applied to EMT as follows:

### 2.1. Rule based

A simple knowledge based heuristic algorithm can be used to determine the position, equivalent diameter, and material type, from a group of three,  
 i. ferromagnetic - iron / steel  
 ii. ferrite  
 iii. conducting / non-magnetic.  
 If the object is approximately circular a few % accuracy can be achieved. This type of algorithm could be used for sorting or sizing material before subsequent separation, e.g. scrap sorting / recycling.

### 2.2. Correlation algorithm

The algorithm correlates the normalised measurement set for each pixel location with the measured values. The correlation coefficient (a value between 0 and 1) is then used as the pixel value [11]. Unfortunately, this approach has limited practical use, possibly for locating the position of known objects. The algorithm has poor spatial sensitivity at the centre of the object space and poor performance with multiple objects.

### 2.3 Back-projection

Back-projection is one of the simplest of the conventional algorithms. This algorithm has been used for a mechanically scanned system [12] but has limited practical use outside of the laboratory.

### 2.4. Sensitivity coefficient and weighted back-projection

These are a widely used algorithm in electrical tomography. With EMT, the images have shown limited central space resolution, which is inherent with soft field system. The results compare very poorly with ART or SIRT.

### 2.5. ART

This algorithm employs an iterative method to overcome the spatial filtering effects of weighted back-projection. New pixel values are up-dated as they are calculated. The iterative step may be described as:

$$f^{(k+1)} = f^{(k)} + I \frac{(p_i - a_i \cdot f^{(k)})}{\|a_i\|^2} a_i^T \quad [5]$$

### 2.6. SIRT

This algorithm is similar to ART, however the new values are up-dated simultaneously as each new image is calculated.

### 2.7. NOSER

The projection matrix is conditioned before the image reconstruction process as described in Table 1, earlier. This technique is as fast as weighted back-projection, but offers similar image quality to SIRT in favourable conditions and when the matrix is appropriately conditioned (i.e. the correct value for  $\mu$ ).

## 2.8. Neural networks

Used to detect faults on metal test objects. The test objects were copper covered cylinders (diameter 4 cm and 5 cm and length 5 cm). Two defects were considered either a vertical or a horizontal gap (0.5 mm or 10 mm) in the copper plating.

## 3. RESULTS

### 3.1. Spatial resolution

One of the tests devised for assessing spatial resolution involved a test object pattern of three parallel aluminium cylinders. This test assesses spatial resolution at the centre of the sensor, which is typically the worst case position. The cylinders were placed at the corners of an equilateral triangle as shown in Figure 3. The distance  $d$  was then increased until the three objects could be clearly distinguished. These particular results were taken from a multi-pole scanner, [13], with an object space diameter of 150 mm.

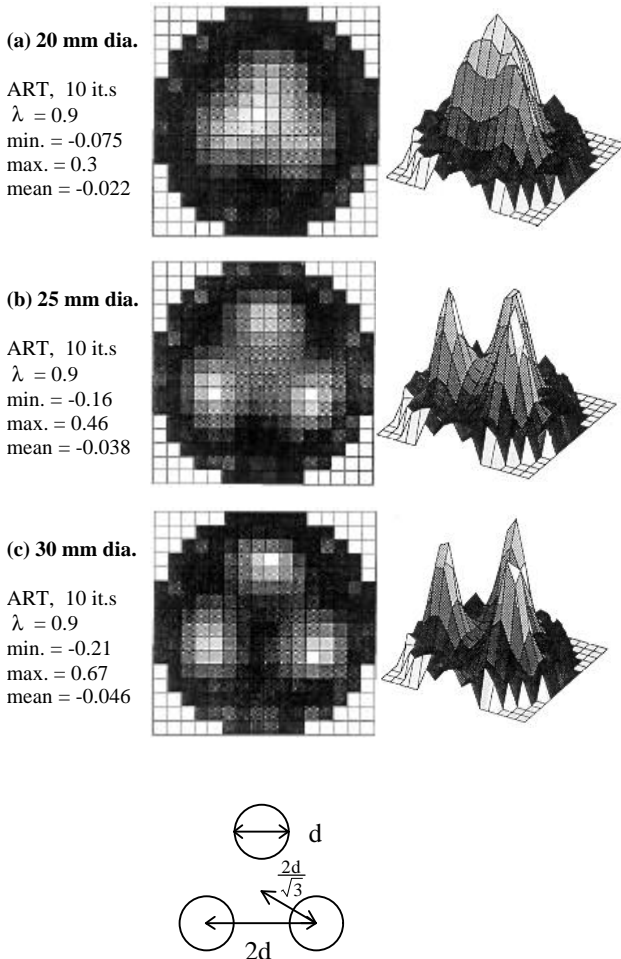


Figure 3. A spatial resolution test using ART

As can be seen the individual bars can be distinguished when distance  $d$  is approximately 15% of the diameter. The optimum value of the relaxation factor,  $\lambda$ , was approximately 0.9, which generally requires in the region of 20 iterations for convergence. Using a lower value of  $\lambda$  will give better noise performance but takes longer to converge. Making use of a priori knowledge can further increase spatial resolution. For example, if the object material is known to be entirely either conductive or magnetic then pixel values can be constrained to be either positive or negative respectively.

### 3.2. Comparison of algorithms

In order to demonstrate the relative merits of the main algorithms, Figure 4 shows images obtained using ART, SIRT, and NOSER and weighted back-projection using three 25 mm aluminium rods. Note, to obtain similar image quality to NOSER, 52 iteration of ART was required without constraining.

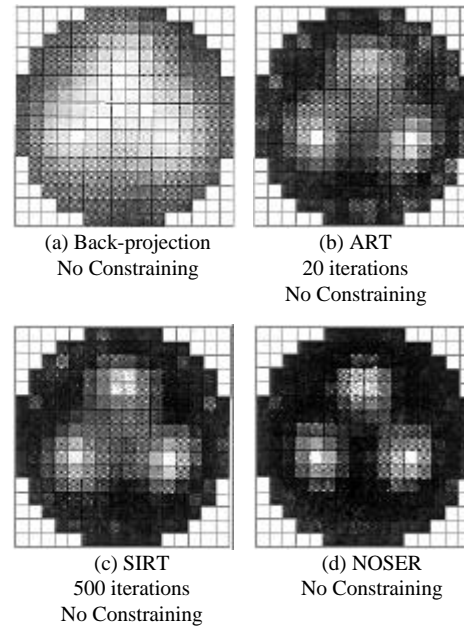


Figure 4. Comparison of several algorithms with 25 mm aluminium rods

Several general conclusions were drawn from the comparison experiments.

- For similar image quality NOSER performs much faster.
- Weighted back-projection performs the least well.
- Relaxation allows ART to perform better in the presence of noise.
- Use of a priori knowledge, such as constraining can increase image quality.

Figure 5 shows how ferrite and conductive material can be distinguished. Figure 5(a) shows three copper bars 15 mm in diameter, which produce positive pixel values. When one of the

bars is changed to ferrite (bottom left), the copper bars still produce positive values but the ferrite produces negative values, shown in Figure 5(b). For copper, the magnetic flux cannot penetrate the object due to induced surface eddy current. The flux must therefore flow around the object. In the case of ferrite, the flux is concentrated in the object as it offers a lower reluctance path. Consequently, copper and ferrite display opposite polarity effects.

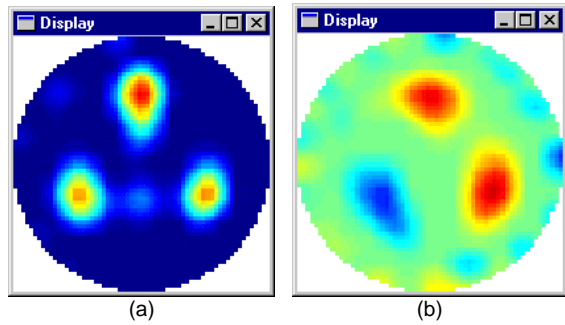


Figure 5. Conductive and magnetic material

### 3.3. Examples

As an example of the potential of this type of tomography, Figure 6 shows an image of steel bars in a concrete pillar. Clearly, the 3 continuous bars are visible, and the discontinuous bar shows up slightly due to the limited axial sensitivity of the sensor. The larger bar can also be identified.

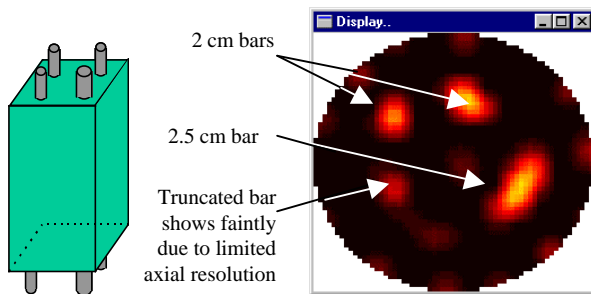


Figure 6. Concrete block with 4 reinforcing bars (one discontinuous); 1x2.5 cm and 2x2 cm.

The final example in Figure 7 shows a sequence of images captured from an agitation and gravitation separation experiment on a simple solid-liquid mixture with a 3 second interval between images. The solid phase is ferrite powder and the liquid phase is water. The EMT system is able to image the distribution of the solid phase because this is the only material in the object space, which is either magnetic or electrically conducting. There is some potential for using this technique to study the operation of solid liquid mixing and separation processes by purposely introducing tracer powder to act as an analogue for one of the phases under investigation. By only introducing a tracer of known particle size it may also be possible to discriminate against particle dimensions.

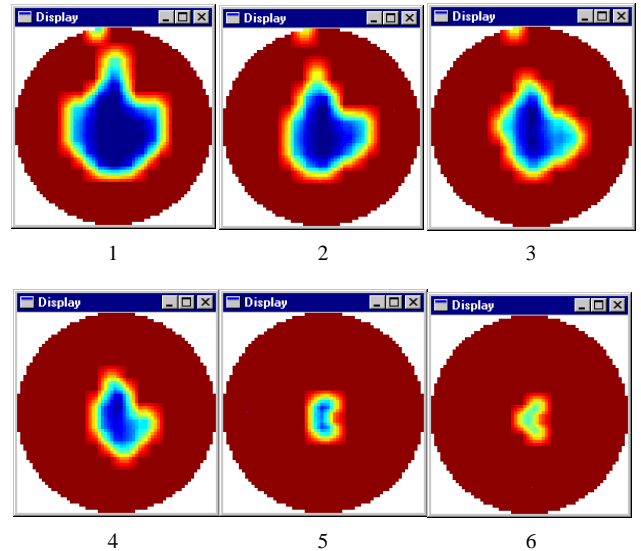


Figure 7. Sequence of images of ferrite powder settling

## 4. SOFTWARE

A modular approach, shown in figure 8, was adopted for the system software, which can be operated in either a UNIX or Windows™ environment and the PC version has been implemented in this study. The system software performs a variety of tasks including control of the data acquisition procedures, image reconstruction, and image visualisation and user interface.

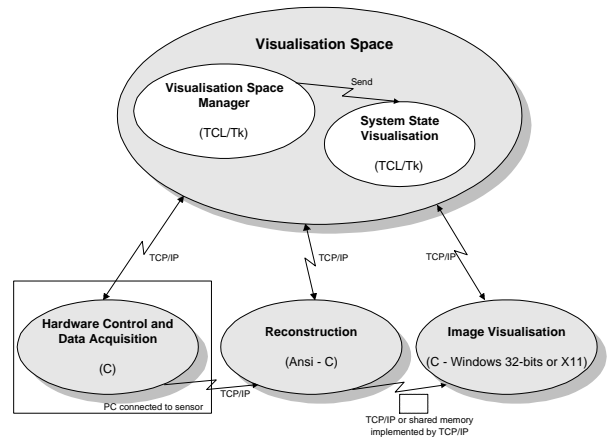


Figure 8. The distributed software framework for EMT

A distributed software framework was developed, for the following reasons:

- i. Speed. A modular and distributed approach enables parallel operation of software modules over several computers.
- ii. Location. The computing hardware that supports the various software functions can be sited in the most appropriate place.
- iii. Future. In a distributed system, the key modules must be clearly structured and

communication protocols fully defined. Consequently, improvements in any one module can be readily incorporated.

During normal operation, the framework has four processes running. Although each of these processes can run independently, they are intended to be part of the framework and the user can control several of their parameters and co-ordinate their execution with the Visualisation Space Manager, VSM. When the VSM is started, the processes for acquisition control (Hwproc), reconstruction (Recproc), and visualisation (Imgproc) are also started. Remproc is started independently. The processes are linked by TCP/IP (Transmission Control Protocol / Internet Protocol) channels so that data and commands can flow, as shown. The VSM was written using TCL/Tk (TCL and the Tk tool kit) which is in the public domain and exists for both UNIX XWindows and PC Windows operating systems. Other processes, including the remote process were developed in C following the ANSI C standard. The choice of TCL/Tk and TCP/IP was driven by the use of ethernet as the communication medium and the desire to produce a framework that could run on both UNIX and MS Windows systems.

## 5. CONCLUSIONS

This paper has described work on a fundamental research project during which a number of EMT imaging systems have been designed built and tested. This has resulted in the development of a modular hardware system and software framework for EMT, which consists of sensor array, control electronics, data acquisition system, high speed computer and image reconstruction software. The maximum excitation frequency for practical operation was also assessed separately for frequencies up to 20 MHz. The performance of the systems has been evaluated with respect to image quality and reconstruction speed. Some initial, but limited, work has also been undertaken to assess the viability of the system for certain industrial applications.

Most of the key issues in understanding how to develop EMT systems for tomographic imaging and what are the performance limitations of these instruments have been addressed. The research has clearly shown the viability of the technique at the fundamental stage of research and substantial foundations have been laid for future applied industrial research on intelligent inductive sensor systems for tomographic imaging and inspection.

## ACKNOWLEDGEMENTS

This work was supported by the European Community through the Brite EuRam programme, project number BE-7961-93, and contract number BRE2-CT94-0604.

## REFERENCES

- [1] C.G. Xie, S.M. Huang, B.S. Hoyle, R. Thorn, C. Lenn, D. Snowden and M.S. Beck, "Electrical capacitance tomography for flow imaging: system model for development of image reconstruction algorithms & design of primary sensors", IEE Proc. G, **139**, pp. 89-98, 1992.
- [2] D.C. Barber, B.H. Brown and I.L. Freeston "Imaging spatial distributions of resistivity using applied potential tomography", Electronics Lett., **19**, pp. 933-5, 1983.
- [3] C.J. Kotre, "A sensitivity coefficient method for the reconstruction of electrical impedance tomograms", Clin. Phys. Physiol. Meas., **11** (Suppl. A), pp. 275-281, 1989.
- [4] G.T. Herman, "Image reconstruction from projections: The fundamentals of computerised tomography", Academic Press, New York, 1980.
- [5] F. Natterer, "The mathematics of computerised tomography", Wiley, Chichester, 1986.
- [6] M.Z. Abdullah, S.V. Quick, and F.J. Dickin, "Quantitative algorithm and computer architecture for real time image reconstruction in process tomography", Proc. 1st ECAPT, pp.170-192., 26-29 March 1992.
- [7] T.J. Yorkey, J.G. Webster, W.J. Tompkins, "An optimal impedance tomographic reconstruction algorithm", Proc. An. Int. Conf. IEEE Eng. Med. Biol. Soc., **8**, pp. 339-42, 1986.
- [8] Ø Isaksen, and Nordtvedt, "A new reconstruction algorithm for process tomography", Meas. Sci. Technol., **4**, pp. 1464-75, 1993.
- [9] W.Q. Yang, J.C. Gamio, M.S. Beck, "A fast iterative image reconstruction algorithm for capacitance tomography", in Sensors and their applications VIII, IOP publishing, Bristol, 1997.
- [10] J. Nuno Lau and A.R. Borges, "Feature detection using electromagnetic tomography and neural networks", IEE colloquium on Advances in Electrical Tomography, Dig. No.

96/143, 19 June 1996.

- [11] Z.Z. Yu, A.J. Peyton, L.A. Xu and M.S. Beck, "*Electromagnetic inductance tomography (EMT): sensor, electronics and image reconstruction for a system with a rotatable parallel excitation field*", IEE Proc. Sci. Meas. Technol., **145**(1), pp. 20-25, 1998.
- [12] S. Al-Zeibak and N.H. Saunders, "*A feasibility study of In Vivo electromagnetic imaging*", Phys. Med. Biol., **38**, pp. 151-60, 1993.
- [13] J. Ferreira, F. Linhares, J. Velez, J. E. de Oliveira, and A.R. Borges, "*Imaging of conductive and ferromagnetic materials using a magnetic induction technique*", 12th annual review of progress in Applied Computational Electromagnetics, pp. 367-374, Monterey Ca. USA, 1996.